Modeling and Validation of the Iodine-Sulfur Hydrogen Production Process

Hanfei Guo, Ping Zhang, Songzhe Chen, Laijun Wang, and Jingming Xu
Nuclear Chemistry and Technology Division, Institute of Nuclear and New Energy Technology, Tsinghua University, Beijing, 100084, P.R. China

DOI 10.1002/aic.14285
Published online November 16, 2013 in Wiley Online Library (wileyonlinelibrary.com)

The iodine-sulfur thermochemical water-splitting cycle (I-S process) is one of the highly efficient, CO_2-free, massive hydrogen production methods. We simulated the I-S process through commercial software programs Aspen Plus and OLI database with the aid of self-developed models to analyze the overall running status of the process and to decrease the investment and time consumption of experiments. A two-phase separator model operating at 353 K and an electro-electrodialysis (EED) cell model working at 338 K were built on the basis of experimental data. The entire flow sheet of the I-S process was modeled based on the two self-developed models. The simulation models were validated through the experimental results obtained from the closed cycle I-S facility (IS-10) in our laboratory. By employing the simulation program, sensitivity analyses of the important parameters in the process were carried out, including the ratio of the distillate to the feed rate of the H_2SO_4 distillation column, reflux ratio of the H_2SO_4 column, H_2SO_4 conversion ratio, HI molality in the EED cathode outlet stream, and HI mole fraction in the liquid and vapor distillates of the HI distillation column. The key parameters significantly affecting the input duty were determined; that is, the ratio of the distillate to the feed rate of the H_2SO_4 distillation column and the HI molality in the EED cathode outlet stream. The optimal values of the analyzed parameters were also discussed. The simulation program we developed is a useful tool that can evaluate and optimize the I-S process. © 2013 American Institute of Chemical Engineers *AIChE J*, 60: 546–558, 2014
Keywords: hydrogen production, iodine-sulfur process, simulation, two-phase separator, electro-electrodialysis

Introduction

Hydrogen is one of the most useful alternative energy carriers because of its numerous advantages. Among the various hydrogen production methods, the iodine-sulfur thermochemical water-splitting cycle (I-S process) is considered one of the most promising, efficient, massive, and CO_2-free approaches. The I-S process, which was initially proposed by the General Atomics company (GA) in the 1970s,[1] can produce hydrogen from water at relatively low temperatures (<1273 K). The efficiency of the I-S process can exceed 40% when coupled with a nuclear reactor, a high-temperature gas-cooled reactor, or a solar plant. The process has been studied by many countries throughout the world, including the United States,[2] Japan,[3] France,[4] Korea,[5] Italy,[6] and China.[7] The I-S process primarily consists of the following three reactions:

Bunsen reaction (exothermic at 293–393 K)

$$SO_2+I_2+2H_2O \rightarrow 2HI+H_2SO_4. \quad (1)$$

Sulfuric acid decomposition (endothermic at 1073–1173 K)

$$H_2SO_4 \rightarrow SO_2+H_2O+1/2O_2. \quad (2)$$

Hydriodic acid decomposition (endothermic at 573–773 K)

$$2HI \rightarrow H_2+I_2. \quad (3)$$

As shown in Figure 1, the I-S process is divided into three sections on the basis of the three reactions: Bunsen, H_2SO_4, and HI sections. In the Bunsen section, HI and H_2SO_4 are produced from H_2O, I_2, and SO_2 through the Bunsen reaction. The mixture of Bunsen products (HI-I_2-H_2SO_4-H_2O) separates into two immiscible liquid phases[8] in the presence of excess iodine, provided that the composition is within an appropriate range.[9] The upper phase (H_2SO_4 phase) comprises a significant amount of H_2SO_4 and a small amount of HI and I_2; the lower phase (HI_x phase, that is, polyhydriodic acid phase) is abundant in HI and I_2 but contains a small amount of H_2SO_4 as well. After separation, the H_2SO_4 and HI_x phases are respectively transported to the H_2SO_4 and HI sections where they undergo purification, concentration, decomposition, and vapor–liquid separation. The reverse reaction (Eq. 4) of the Bunsen reaction is utilized in the purification subsection to eliminate the impurities of the two phases, which are H_2SO_4 in the HI_x phase and HI and I_2 in the H_2SO_4 phase.[10,11] The distillation columns and condensers are proposed in the concentration and vapor–liquid separation subsections, respectively. The gaseous outlet streams of the vapor–liquid separations are H_2 and O_2. The liquid outlet streams are returned to the Bunsen section to participate in the Bunsen reaction. As a result, the net inputs of the I-S process are water and high-temperature heat, and the net outputs are H_2, O_2, and low-temperature heat; the other materials are recycled constantly

$$2HI+H_2SO_4 \rightarrow SO_2+I_2+2H_2O \quad (4)$$

Correspondence concerning this article should be addressed to Ping Zhang at zhangping77@tsinghua.edu.cn.

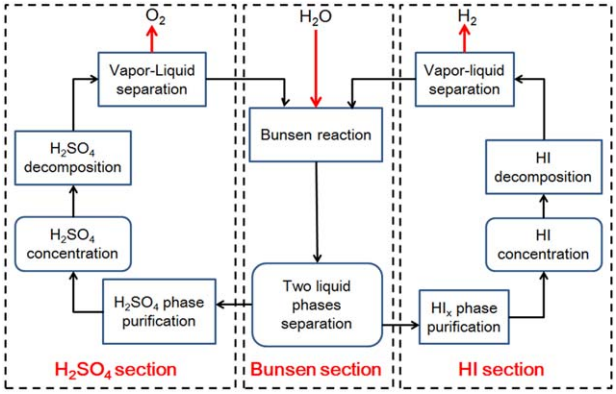

Figure 1. Schematic flow sheet of the I-S process.

[Color figure can be viewed in the online issue, which is available at wileyonlinelibrary.com.]

Considering that the HI-I_2-H_2O (HI_x) mixture that needs to be concentrated in the HI section exhibits azeotropy,[12] high-concentration HI cannot be obtained through conventional distillations in the HI concentration subsection (Figure 1). Therefore, special distillations or preconcentration means should be employed. Recently, three methods have been extensively investigated, namely, extractive distillation using H_3PO_4 as the extraction agent,[8] reactive distillation,[13] and distillation with an electro-electrodialysis (EED) cell for preconcentration.[14]

Research on the I-S process has been intensively conducted in the Institute of Nuclear and New Energy Technology (INET), Tsinghua University of China. The flow sheet with an EED cell for the preconcentration of the HI_x mixture is adopted, and a principle verification facility (IS-10) with H_2 production of 10 NL/h was constructed and successfully operated.[15] The experimental IS-10 facility in INET is shown in Figure 2.

Figure 3 presents the flow sheet of the I-S process involving an EED cell. The flow sheet indicates that the process is complex and contains many reactors, columns, separators, and heat exchangers. The three sections are highly coupled by a number of recycled streams. Thus, the overall running status of the process is difficult and expensive to determine by using mere experimental approaches. Simulation must be employed to investigate the process, determine the key parameters through sensitivity analysis, and establish optimization to improve efficiency.

Giaconia et al.[16] and Huang and T-Raissi[17] carried out simulation studies on the H_2SO_4 section with Aspen Plus and HYSYS, respectively. Giaconia et al.[16] proposed a series of four evaporators to concentrate H_2SO_4, and Huang and T-Raissi[17] investigated the kinetics of the decomposition of H_2SO_4 in detail. Goldstein et al.,[4] Belaissaoui et al.,[18] Elder et al.,[19] Kane and Revankar,[20] and Murphy and O'Connell[21] examined the performance of the HI section and adopted reactive distillation columns to concentrate and decompose HI. Kasahara et al.[22] and Guo et al.[23,24] established a model for the EED cell, built a flow sheet for the simulation of the HI section that involved the EED for the preconcentration of HI and analyzed the energy requirement of the flow sheet. Mathias and Brown[25,26] updated the electrolyte nonrandom two-liquid thermodynamic model and simulated the entire flow sheet of the I-S process by means of the updated model. A reactive distillation column was adopted in their flow sheet for the HI section. However, the phase separation behavior of the Bunsen products could not be predicted reliably. Kasahara et al.[27,28] also simulated the flow sheet of the entire I-S process by applying the EED cell to the HI section. They determined the HI molality of the EED cathode outlet stream to be the key parameter of total duty through sensitivity analysis. However, several process units were not modeled rigorously in their calculation but were computed on the basis of assumptions or experimental experience, such as the two-phase separator in the Bunsen section and the EED. More research is needed to improve the content and the predictability of the simulation model.

In summary, although a number of studies have reported simulations of the H_2SO_4 and HI sections, simulations of the entire flow sheet of the I-S process are relatively few. The published simulation model of the overall flow sheet is incomplete.

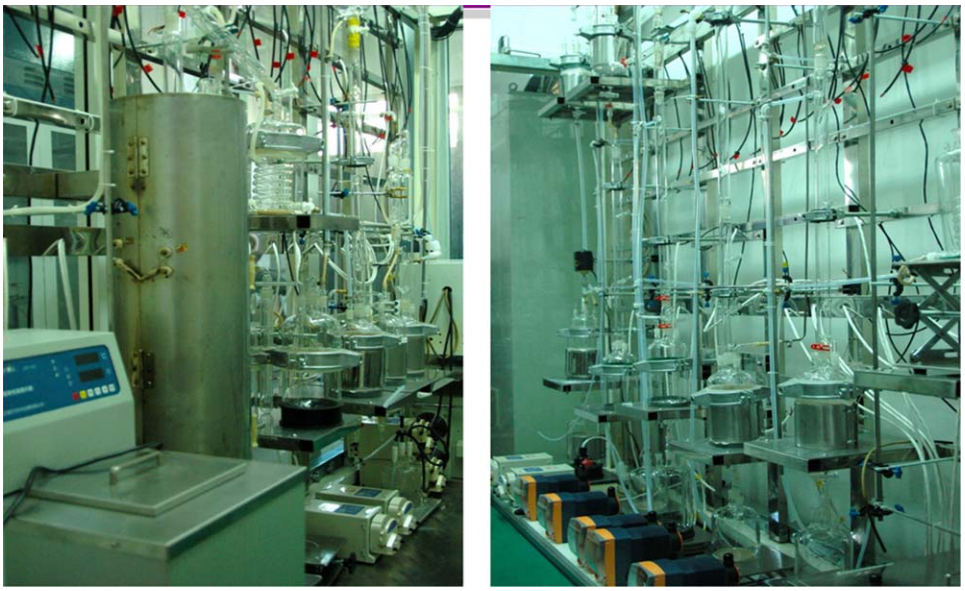

Figure 2. Experimental facility of IS-10 in Institute of Nuclear and New Energy Technology (INET), Tsinghua University.

[Color figure can be viewed in the online issue, which is available at wileyonlinelibrary.com.]

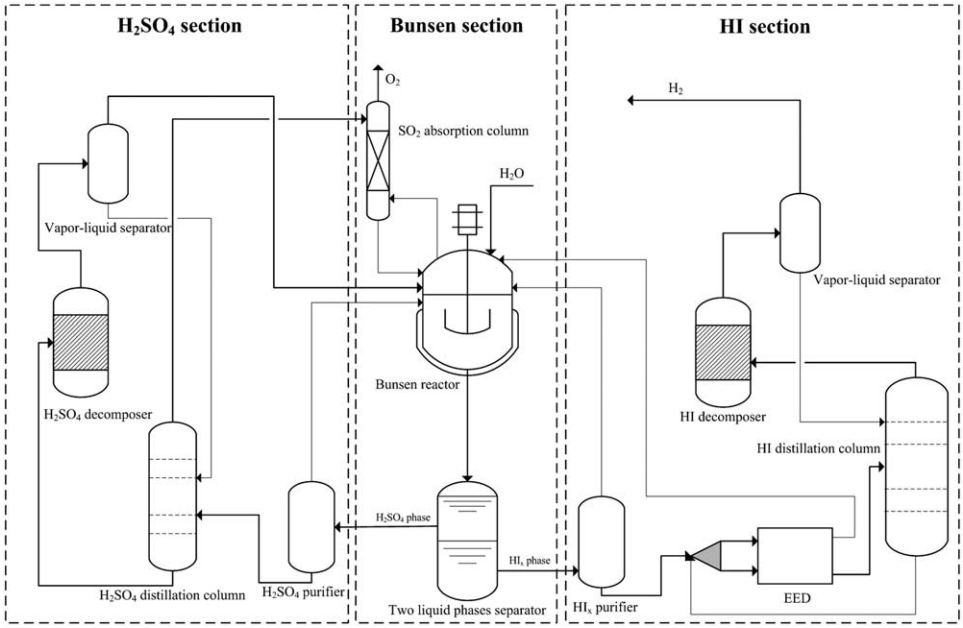

Figure 3. Flow sheet of the I-S process with an EED cell.

This study aims to build a complete simulation model for the entire I-S process, on the basis of the experimental analyses and calculations we have carried out in INET. The two self-developed models, that is, the two-phase separator for the Bunsen section and the EED, were established. Subsequently, the entire flow sheet for the simulation was created and validated through the experimental data obtained from the IS-10 facility. Finally, sensitivity analyses were conducted to evaluate the influences of the important parameters on input duty. The optimal values for these parameters were also determined.

Simulation Model and Parameter Analysis

Modeling the I-S process

The commercial software programs Aspen Plus (version 7.2, Aspen Technology) and OLI database (version 8.2, OLI Systems) were adopted for the simulation. Most of the operation units in the I-S process can be modeled by the blocks that the software possesses. However, extreme difficulty was encountered in modeling the phase separator in the Bunsen section and the EED cell in the HI section because the thermodynamic database of the simulation software is incapable of predicting the phase separation behavior of the Bunsen product. In addition, Aspen Plus cannot simulate the electrochemical processes. As a result, custom models for the phase separator and EED have to be developed on the basis of experimental data.

Simulation model of the phase separator in the Bunsen section

The Bunsen product, which is comprised of HI, I_2, H_2SO_4, and H_2O, separates into two liquid phases when the composition of the mixture is within an appropriate range at a definite temperature. Hadj-Kali et al.[29] proposed a thermodynamic model to predict the liquid–liquid-phase equilibrium behavior of the Bunsen products. The main assumptions of the model were acids total dissociation and total H^+

Table 1. Liquid–Liquid-Phase Equilibrium Data (Mole Fraction) at 353 K

Feed				HI_x Phase				H_2SO_4 Phase			
x^{fd}_{HI}	$x^{fd}_{I_2}$	x^{fd}_{SA}	$x^{fd}_{H_2O}$	x^{hi}_{HI}	$x^{hi}_{I_2}$	x^{hi}_{SA}	$x^{hi}_{H_2O}$	x^{sa}_{HI}	$x^{sa}_{I_2}$	x^{sa}_{SA}	$x^{sa}_{H_2O}$
0.12	0.06	0.12	0.70	0.18	0.31	0.00	0.51	0.01	0.01	0.14	0.84
0.10	0.05	0.21	0.64	0.12	0.31	0.02	0.55	0.00	0.00	0.21	0.79
0.09	0.05	0.27	0.59	0.05	0.24	0.01	0.70	0.00	0.00	0.08	0.92
0.11	0.11	0.11	0.67	0.14	0.26	0.01	0.59	0.01	0.00	0.17	0.83
0.09	0.09	0.19	0.63	0.26	0.74	0.00	0.00	0.00	0.00	0.13	0.87
0.09	0.09	0.26	0.56	0.20	0.79	0.01	0.00	0.00	0.00	0.29	0.71
0.09	0.19	0.09	0.63	0.13	0.40	0.02	0.45	0.00	0.00	0.27	0.73
0.09	0.17	0.17	0.57	0.23	0.77	0.00	0.00	0.00	0.00	0.14	0.86
0.08	0.15	0.19	0.58	0.21	0.79	0.00	0.00	0.00	0.00	0.14	0.86
0.08	0.25	0.08	0.59	0.22	0.78	0.00	0.00	0.00	0.00	0.14	0.86
0.12	0.06	0.06	0.76	0.26	0.32	0.02	0.40	0.01	0.01	0.11	0.87
0.13	0.04	0.08	0.75	0.19	0.20	0.01	0.60	0.01	0.00	0.10	0.89
0.13	0.06	0.05	0.76	0.38	0.56	0.06	0.00	0.04	0.01	0.08	0.87
0.13	0.03	0.09	0.75	0.12	0.16	0.02	0.70	0.04	0.02	0.03	0.91
0.03	0.20	0.03	0.74	0.23	0.75	0.02	0.00	0.00	0.00	0.14	0.86
0.12	0.06	0.04	0.78	0.20	0.17	0.04	0.59	0.08	0.04	0.11	0.77

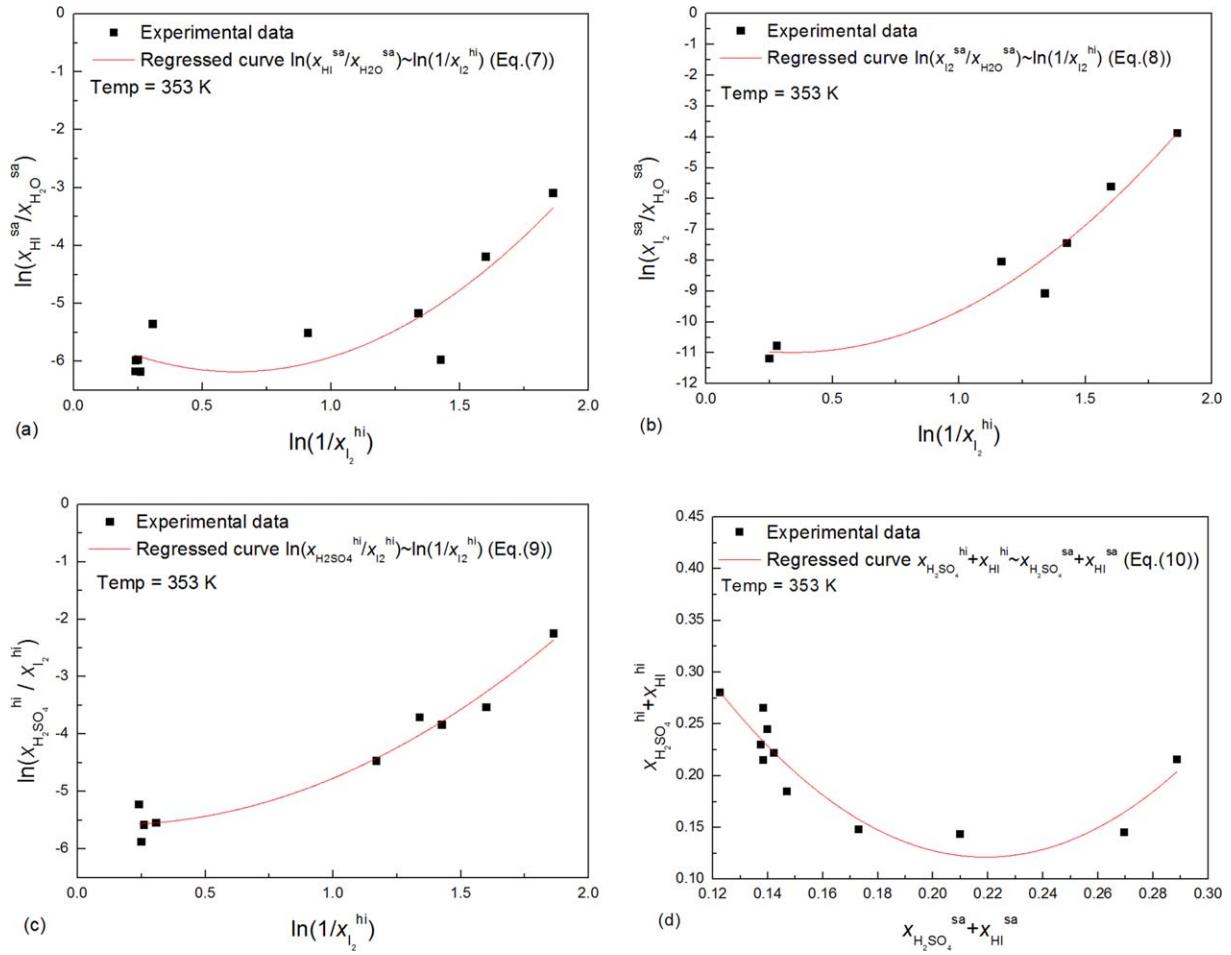

Figure 4. Regression results of the liquid-liquid equilibrium of the Bunsen products at 353 K.

[Color figure can be viewed in the online issue, which is available at wileyonlinelibrary.com.]

solvation by water. However, implementing this model in the process simulation is inconvenient due to the difficulty in solving the model equations.

We studied the demixing characteristics of the Bunsen products at 293 K in our previous work,[9] and determined the composition range within which the mixture could separate into two immiscible liquid phases. In this study, we continue to investigate the liquid–liquid-phase equilibrium property of the mixture at 353 K to simulate the phase separator in the flow sheet of the Bunsen section because the actual operating temperature of the phase separator is 353 K.[15]

The experimental data of the liquid–liquid-phase equilibrium at 353 K and the feed compositions are shown in Table 1. In this experiment, the HI-I_2-H_2SO_4-H_2O mixture (feed) was prepared in a 25-mL test tube with a plug. The test tube was then placed in a thermostatic water bath, in which the temperature was maintained at 353 K. When the solution separated into two liquid phases, it was kept at rest until the droplets transferring between the two liquid phases could no longer be observed (about 0.5–2 h). Afterward, the plug of the tube was removed, and the upper (H_2SO_4 phase) and lower phases (HI_x phase) were sampled by using a rubber head dropper, respectively. The samples were weighted on an analytical balance (1/1000), and the composition and density of the samples were measured. The concentrations of H^+, I_2, and I^- were determined by potential titration with NaOH, $Na_2S_2O_3$, and KIO_3, respectively. The measurement errors were less than 0.5%. The concentration of SO_4^{2-} was measured by ion chromatography (Dionex ICS-2100) with an IonPac AG20 guard column and an IonPac AS20 separation column. An electrical conductivity detector and a KOH elution instrument were utilized in ion chromatography. The concentration of the elution varied between 10 and 50 mmol/L (gradient elution), and the flow rate of the elution was 1.0 mL/min. The measurement error was less than 5%. The density of the sample was determined with a density meter (DMA-4500, Anton Paar, Austria) with a measurement error of 0.0001 g/cm^3. The concentration of water was calculated based on the relation between density and the composition of the mixture (Eq. 5)

$$\rho = C_{HI} \cdot M_{HI} + C_{I_2} \cdot M_{I_2} + C_{H_2SO_4} \cdot M_{H_2SO_4} + C_{H_2O} \cdot M_{H_2O} \quad (5)$$

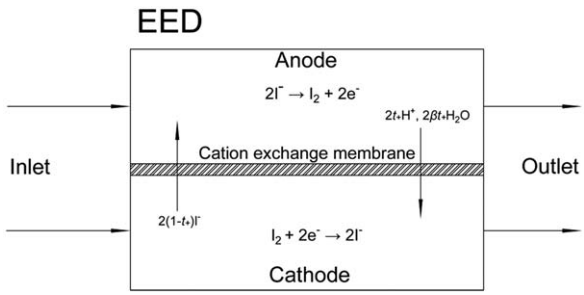

Figure 5. Functional diagram of EED.

Table 2. Comparison of the Calculated EED Voltage by Eq. 17 with Experimental Data at 338 K

Concentration				Experimental EED Voltage (V)	Calculated EED Voltage (V)
x_{HI}^{ca}	$x_{I_2}^{ca}$	x_{HI}^{an}	$x_{I_2}^{an}$		
0.12	0.13	0.12	0.13	0.515	0.520
0.13	0.10	0.12	0.14	0.627	0.615
0.13	0.07	0.10	0.14	0.774	0.785
0.14	0.07	0.09	0.17	0.906	0.901

The relative analytical error of water concentration is less than 10% when the water mole fraction is greater than 0.40. The relative error may grow larger when the water content is quite low (close to zero), but the absolute error is still small (less than 0.06). A few water mole fractions in the HI_x phase reported in Table 1 equal to zero. It is possible that for some cases, the actual water mole fraction is greater than zero (but less than 0.06), and the reported zero mole fraction is due to the analytical error. However, this error range of water concentration in the HI_x phase almost does not affect the accuracy of the regression equations (Eqs. 7–10) thereinafter.

The chemical potential of a component in one phase equals that in the other phase when the two phases reach equilibrium.[30] Thus, the following four relations for the mixture of the Bunsen products are deduced

$$\mu_{HI}^{hi}=\mu_{HI}^{sa};\ \mu_{I_2}^{hi}=\mu_{I_2}^{sa};\ \mu_{H_2SO_4}^{hi}=\mu_{H_2SO_4}^{sa};\ \mu_{H_2O}^{hi}=\mu_{H_2O}^{sa}. \quad (6)$$

However, the chemical potential of the concentrated electrolyte solutions is difficult to calculate accurately. Therefore, we regressed our experimental data in Table 1 and obtained the following equations for the liquid–liquid equilibrium at 353 K

$$\ln\left(\frac{x_{HI}^{sa}}{x_{H_2O}^{sa}}\right)=a_1\cdot\left(\ln\frac{1}{x_{I_2}^{hi}}\right)^2+b_1\cdot\left(\ln\frac{1}{x_{I_2}^{hi}}\right)+c_1 \quad (7)$$

$$\ln\left(\frac{x_{I_2}^{sa}}{x_{H_2O}^{sa}}\right)=a_2\cdot\left(\ln\frac{1}{x_{I_2}^{hi}}\right)^2+b_2\cdot\left(\ln\frac{1}{x_{I_2}^{hi}}\right)+c_2 \quad (8)$$

$$\ln\left(\frac{x_{H_2SO_4}^{hi}}{x_{I_2}^{hi}}\right)=a_3\cdot\left(\ln\frac{1}{x_{I_2}^{hi}}\right)^2+b_3\cdot\left(\ln\frac{1}{x_{I_2}^{hi}}\right)+c_3 \quad (9)$$

$$x_{HI}^{hi}+x_{H_2SO_4}^{hi}=a_4\cdot\left(x_{HI}^{sa}+x_{H_2SO_4}^{sa}\right)^2+b_4\cdot\left(x_{HI}^{sa}+x_{H_2SO_4}^{sa}\right)+c_4. \quad (10)$$

The symbols a_i, b_i, c_i ($i=1$–4) are the regression coefficients.

Figure 4 shows the regression results and experimental data. The experimental error is within ±5%. The relative errors between the calculated and experimental values in Figures 4a–d are 6.3, 5.4, 4.0, and 6.1%, respectively.

To calculate the composition of the two liquid phases, mass-balance equations and normalization equations were used.

The mass-balance equations are as follows

$$X_{HI}=R^{hi}\cdot x_{HI}^{hi}+R^{sa}\cdot x_{HI}^{sa} \quad (11)$$

$$X_{I_2}=R^{hi}\cdot x_{I_2}^{hi}+R^{sa}\cdot x_{I_2}^{sa} \quad (12)$$

$$X_{H_2SO_4}=R^{hi}\cdot x_{H_2SO_4}^{hi}+R^{sa}\cdot x_{H_2SO_4}^{sa} \quad (13)$$

$$X_{H_2O}=R^{hi}\cdot x_{H_2O}^{hi}+R^{sa}\cdot x_{H_2O}^{sa}. \quad (14)$$

The normalization equations are as follows

$$x_{HI}^{hi}+x_{I_2}^{hi}+x_{H_2SO_4}^{hi}+x_{H_2O}^{hi}=1 \quad (15)$$

$$x_{HI}^{sa}+x_{I_2}^{sa}+x_{H_2SO_4}^{sa}+x_{H_2O}^{sa}=1. \quad (16)$$

The model of the phase separator is built based on the above equations. When the overall composition of the Bunsen products is provided at 353 K, the composition and proportion of the two liquid phases can be predicted by solving Eqs. 7–16 simultaneously.

Simulation model of the EED cell

EED aims to improve the concentration of HI in the HI-I_2-H_2O solution to that of over azeotrope with the aid of electricity. The working principle of the EED cell is presented in Figure 5. We established the mass-balance equations in our previous study[24] according to the operating principle.[31,32] When the flow rate and composition of the inlet streams are provided, the parameters of the outlet streams are determined by the mass-balance equations.[24]

The EED experimental data were regressed to relate the voltage of EED and the composition of the anolyte and catholyte. The experimental data (experimental error is within ±2%) obtained from INET were utilized for the regression. The result is expressed by Eq. 17. Table 2 compares the EED voltages calculated by Eq. 17 with the experimental data

$$E=0.5204-0.2661\cdot\ln\left(\frac{x_{I_2,mn}^{ca}}{x_{I_2,mn}^{an}}\right)+0.3567\cdot\ln\left(\frac{x_{HI,mn}^{ca}}{x_{HI,mn}^{an}}\right) \quad (17)$$

Table 2 indicates that the results calculated by Eq. 17 fits the experimental data. Thus, the EED model was built. In the simulation, most of the calculated HI and I_2 mole fractions were within the variation range of the experimental data used for regression in Eq. 17. In the sensitivity analysis of HI molality in the EED cathode outlet stream, a few high-concentration HI data were calculated by extrapolating Eq. 17.

Simulation model of the global I-S process

When the phase separator model and EED cell model were made, the flow sheet of the entire I-S process was established with Aspen Plus because the other process units in the flow sheet can be simulated by the modules that Aspen software contains. The flow sheet established by the simulation software is shown in Figure 6.

The Bunsen section includes three main units: the Bunsen reactor R-101, phase separator S-102, and SO_2 absorber T-104. A-103 is a mixer, and P-407 and P-408 are pumps. The process units in the H_2SO_4 section gather on the left side of Figure 6, including H_2SO_4-phase purifier R-202, H_2SO_4 distillation column T-204, H_2SO_4 decomposer R-207, vapor–liquid separator E-208, and heat exchanger E-210. On the right side of figure are the units of the HI section, primarily

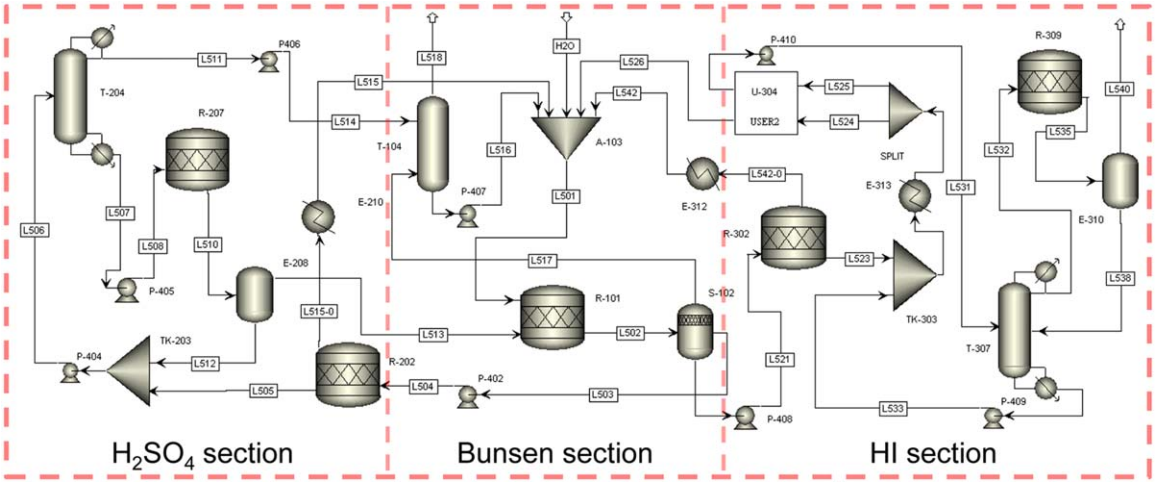

Figure 6. Flow sheet of the I-S process in Aspen Plus.

[Color figure can be viewed in the online issue, which is available at wileyonlinelibrary.com.]

Table 3. Specified Parameters for the Process units in the Simulation of IS-10 Facility

Process Unit	Parameters
SO_2 absorber (T-104)	Three stages, no condenser or reboiler, 0.1 MPa
Bunsen reactor (R-101)	353 K, 0.1 MPa, SO_2 conversion 100%
Vapor–liquid–liquid separator (S-102)	0.1 MPa, heat duty = 0
H_2SO_4 phase purifier (R-202)	403 K, 0.1 MPa, HI conversion 98%
H_2SO_4 distillation column (T-204)	Five stages, feed at stage 3, reflux ratio = 1, distillate rate/feed rate = 0.72, 0.1 MPa
H_2SO_4 decomposer (R-207)	1123 K, 0.1 MPa, H_2SO_4 conversion 78%
Vapor–liquid separator (E-208)	333 K, 0.1 MPa
Condenser (E-210)	0.1 MPa, vapor fraction of the outlet stream = 0
HI_x-phase purifier (R-302)	393 K, 0.1 MPa, H_2SO_4 conversion 97%
Heat exchanger (E-313)	Temperature of outlet stream = 338 K, 0.1 MPa
Splitter (SPLIT)	Ratio of the molar flow rates of the outlet streams = 1/1
EED (U-304)	Effective membrane area = 800 cm^2, $t_+ = 0.96$, $\beta = 1.65$, temperature = 338 K, current density = 74 A/m^2, voltage = 0.542 V
HI distillation column (T-307)	Seven stages, feed at stage 4, reflux ratio = 0.5, 0.1 MPa, distillate rate/feed rate = 0.8
HI decomposer (R-309)	723 K, 0.1 MPa, HI conversion 21%
Vapor–liquid separator (E-310)	313 K, 0.1 MPa
Condenser (E-312)	0.1 MPa, vapor fraction of the outlet stream = 0

composed of the HI_x-phase purifier R-302, EED U-304, HI distillation column T-307, HI decomposer R-309, vapor–liquid separator E-310, and heat exchanger E-312.

After phase separation in the Bunsen section, the upper phase (H_2SO_4 phase) stream L503 is sent to the H_2SO_4 section, and the lower phase (HI_x phase) stream L521 flows to the HI section. The H_2SO_4 section returns streams L513, L514, and L515 to the Bunsen section, which are the vapor outlet stream of separator E-208, the distillate of column T-204, and the vapor outlet stream of purifier R-202, respectively. The HI section returns streams L526 and L542 to the Bunsen section. L526 and L542 are the anode outlet stream of EED and the vapor outlet stream of purifier R-302, respectively. Although L515 and L542 are vapor streams from purifiers R-202 and R-302, they reach the mixer A-103 as liquids after undergoing heat exchange.

Validation of the simulation model using experimental data

The experimental data[15] obtained from the operation of the IS-10 facility were utilized to validate the reliability of the simulation model. During the simulation of the IS-10

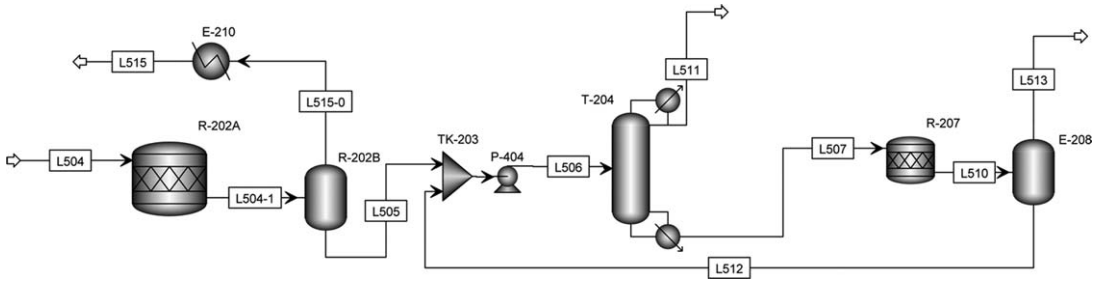

Figure 7. Flow sheet of H_2SO_4 section for sensitivity analysis.

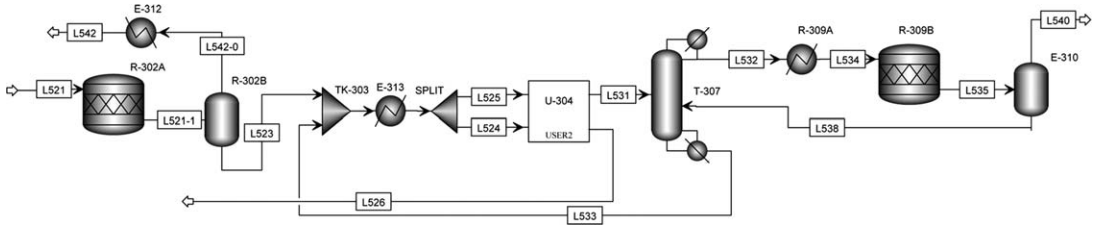

Figure 8. Flow sheet of HI section for sensitivity analysis.

facility, the specified parameters of the process units and the arrangement of the internal circuits in the model were set as close to the actual case as possible. The specified parameters are listed in Table 3.

The calculated parameters of the key streams in the flow sheet were compared with the experimental data, including the H_2 and O_2 production rates, the compositions of the outlet streams of the EED, the HI distillation column, the H_2SO_4 distillation column, and the compositions of the recycled key streams.

Parameter analysis of the flow sheets of the H_2SO_4 section and HI section

The influence of the important parameters on the energy requirement was analyzed to optimize the operating parameters and reduce the heat duty. Given that the Bunsen section does not demand input heat, we concentrated on the H_2SO_4 and HI sections. The examined flow sheets of the H_2SO_4 and HI sections are depicted in Figures 7 and 8. The HI decomposer in Figure 8 is divided into two virtual units R-309A and R-309B for the convenience of calculation. The distillate L532 is heated to the specified reaction temperature in R-309A, then sent to R-309B where reaction takes place. The combination of R-309A and R-309B is equivalent to an actual HI decomposer.

The evaluated parameters in the H_2SO_4 section were the ratio of distillate rate to feed rate of the H_2SO_4 distillation column, reflux ratio, and the H_2SO_4 conversion ratio in the decomposer. The evaluated parameters in the HI section were HI molality in the EED cathode outlet stream, HI mole fraction in the liquid distillate, and HI mole fraction in the vapor distillate of the HI distillation column. The variation range and basic value of each parameter are presented in Table 4. When one parameter is being analyzed, the others are fixed at their respective basic values. The basic value of a parameter is the median of its variation range or the estimated optimal value for the parameter.

During the analysis, all the other parameters except those that were evaluated were fixed. The specified values were determined by reference to the experimental data[7,15] or calculated results[23,33] in our previous research (Tables 5 and 6).

Table 4. Evaluated Parameters

Parameter	Variation Range	Basic Value
Distillate rate to feed rate of H_2SO_4 distillation column	0.4–0.85	0.75
Reflux ratio of H_2SO_4 distillation column	0.1–5.0	1.0
H_2SO_4 conversion ratio	0.55–0.95	0.75
HI molality in EED cathode outlet stream (mol/kg-H_2O)	10.20–12.15	11.05
HI mole fraction in liquid distillate of HI distillation column	0.19–0.35	0.23
HI mole fraction in vapor distillate of HI distillation column	0.2–0.6	0.3

Results and Discussion

Validation of the simulation model

Validation of the Simulation Model of Phase Separator. The experimental data in the literature[34,35] and in our study (Table 1) were employed to validate the phase separator model. The experimental overall composition of the mixture was input, and the composition and amount of the two immiscible liquid phases calculated by the model were compared with the experimental data, as shown in Figures 9 and 10. The symbol R^{hi} was adopted to denote the molar ratio of the HI_x phase to the mixture of the Bunsen product, and the accuracy of the calculated amounts of the two immiscible liquid phases was examined by validating the value of R^{hi} (Figure 10).

Figure 9 indicates that the absolute value of the mean relative error between the calculated and experimental data is 11.0%; in Figure 10, the error is 11.7%. The errors of the experimental data in Figures 9 and 10 are within ±5%. The calculated values fit the experimental data; thus, the phase separator model is valid. This model is extremely significant because it solves the problem of predicting the phase separation behavior and the compositions of the two immiscible phases of the Bunsen products. It is the key point for completing the simulation of the overall I-S process.

Validation of the Simulation Model of the Global Flow Sheet. The IS-10 facility was simulated with the model. The flow sheet is illustrated in Figure 11. The internal circuits of the HI section in IS-10 are different from that shown in Figure 6. In Figure 11, the recycled streams L533 (bottom product of the column T-307), L538 (liquid outlet stream of the V-L separator E-310), and L526 (EED anode outlet stream) are returned to A-103 (mixer of the Bunsen section), TK-303 (mixer of the HI section), and R-202 (HI_x-phase

Table 5. Fixed Parameters in the Sensitivity Analysis of H_2SO_4 Section

Parameter Type	Parameter Value
Feed composition (L504)	$HI/I_2/H_2SO_4/H_2O$ = 0.006/0.003/0.150/0.841
Purification reactor (R-202A)	403 K, 0.1 MPa, HI conversion ratio = 100%
Purification separator (R-202B)	0.1 MPa, heat duty = 0
Distillation column (T-204)	Five stages, feed at the third stage, 0.1 MPa
Decomposer (R-207)	1123 K, 0.1 MPa
V-L separator (E-208)	333 K, 0.1 MPa
Condenser (E-210)	0.1 MPa, vapor fraction of the outlet stream = 0

Table 6. Fixed Parameters in the Sensitivity Analysis of HI Section

Parameter Type	Parameter Value
Feed composition (L521)	$HI/I_2/H_2SO_4/H_2O$ = 0.099/0.161/0.007/0.733
Purification reactor (R-302A)	393 K, 0.1 MPa, H_2SO_4 conversion ratio = 95%
Purification separator (R-302B)	0.1 MPa, heat duty = 0
Heater (E-313)	Temperature of outlet stream = 338 K, 0.1 MPa
Splitter (SPLIT)	Ratio of the molar flow rates of the outlet streams = 1/1
EED (U-304)	Effective membrane area = 800 cm^2, $t_+ = 0.96$, $\beta = 1.65$, temperature = 338 K
Distillation column (T-307)	Seven stages, feed at the fourth stage, reflux ratio 0.1, 0.1 MPa
Preheater (R-309A)	Temperature of outlet stream = 723 K, 0.1 MPa
Decomposer (R-309B)	723 K, 0.1 MPa, HI conversion ratio = 21%
V-L separator (E-310)	313 K, 0.1 MPa
Condenser (E-312)	0.1 MPa, vapor fraction of the outlet stream = 0

purifier), respectively. However, in Figure 6, these three recycled streams are returned to TK-303, T-307, and A-103, respectively. The flow sheet presented in Figure 6 is more energy-efficient than the flow sheet in Figure 11 on the basis of our recent study.[24] However, when the experimental data for the present validation were obtained, the flow sheet in Figure 11 was employed for the IS-10 facility. In the succeeding sections of parameter analysis in this article, the arrangement of the circuits in the HI section will be adjusted to that displayed in Figure 6.

When the simulation converged, the calculated parameters for the streams were summarized. The results are shown in Table 7.

The calculated flow rates of the produced H_2 and O_2 were compared with the experimental data in Table 8. Table 9 compares the set values of the conversion ratio and removal ratios of HI and H_2SO_4 with the experimental results. The calculated and experimental compositions of the key streams are compared in Tables 10–12. As for the experimental data in Tables 10 and 12, the error of the analytical method is within ±5%, but the sampling procedure may give rise to more errors due to the issue of iodine vapor escaping or iodine precipitation.

The hydrogen and oxygen production rates are the most important parameters in the hydrogen production process. In the actual operation of the IS-10 facility, the flow rates of the produced hydrogen and oxygen fluctuate in a small range (Table 8), and so do the conversion ratios of HI and H_2SO_4 in the decomposers and removal ratios of the two acids in the purifiers (Table 9). As shown in Tables 8 and 9, all the computed flow rates of H_2 and O_2 as well as the conversion and removal ratios of HI and H_2SO_4 lie within the variation range of the experimental results.

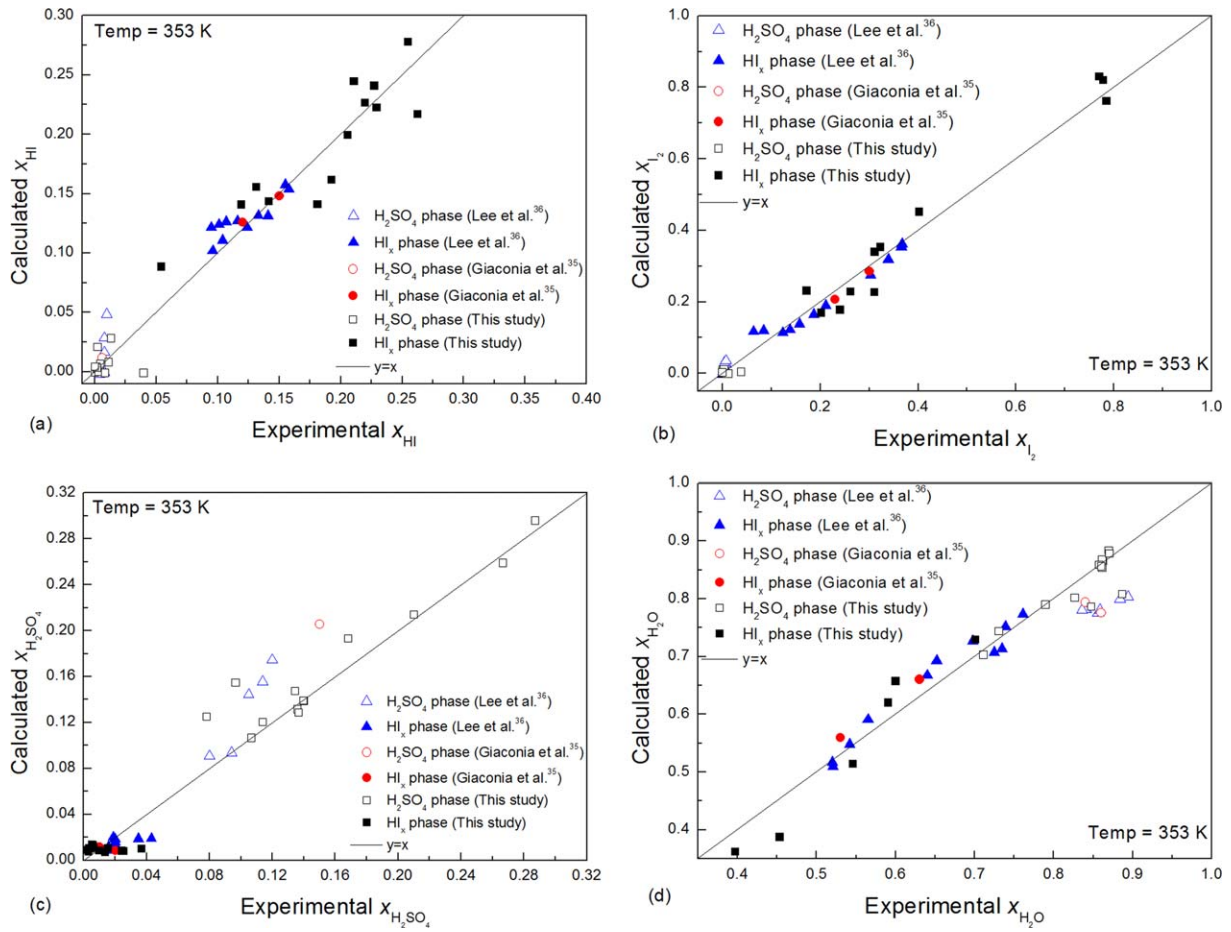

Figure 9. Comparison of the calculated compositions of the HI_x and H_2SO_4 phases with experimental data at 353 K.

(a) mole fraction of HI; (b) mole fraction of I_2; (c) mole fraction of H_2SO_4; and (d) mole fraction of H_2O. [Color figure can be viewed in the online issue, which is available at wileyonlinelibrary.com.]

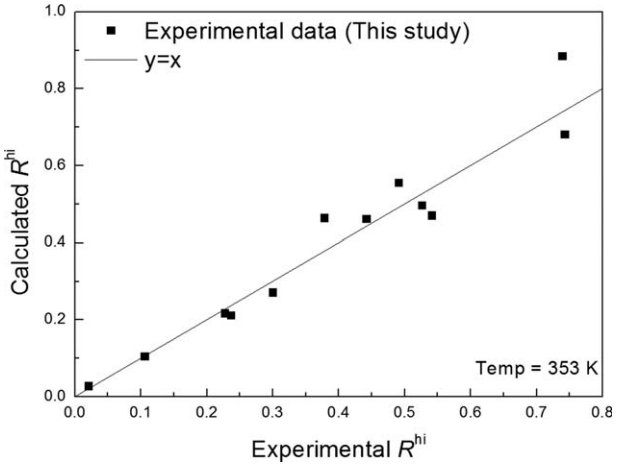

Figure 10. Comparison of the calculated R^{hi} (molar ratio of the amount of HI_x phase to the mixture) with the experimental data at 353 K.

The HI distillation column, H_2SO_4 distillation column, and EED are the three key process units. The two distillation columns feed the HI and H_2SO_4 decomposer, respectively; thus, the compositions of the outlet streams of the two columns significantly influence the flow rates of H_2 and O_2. Given that the EED cathode outlet stream feeds the HI distillation column, the composition of this stream greatly affects the mass and heat balance in the column. Clearly, the two columns and EED are very important process units, and their outlet streams are key streams, specifically the EED cathode outlet stream (L531), the distillate of the HI distillation column (L532), and the bottom product of the H_2SO_4 distillation column (L507). Table 10 shows that most of the calculated compositions of L531 and L532 fit the experimental results well, and Table 11 indicates that the calculated mass fraction of H_2SO_4 in L507 lies within the variation range of the experimental data. The error between the calculated and experimental iodine mole fractions of stream L531 resulted from the measurement error. The low content of iodine in L531 and the relatively small sample volume led to the increase in measurement error of titration. However, the error between the calculated and experimental iodine mole fractions is not significant; thus, the calculated results still coincide with the experimental data.

With regard to the recycled streams, the bottom product of the HI distillation column (L533) has the largest flow rate among all the circuit streams; hence, the stream L533 significantly influences the mass balance of the Bunsen section. The HI_x phase (L521) and H_2SO_4 phase (L503) of the Bunsen product feed the HI section and H_2SO_4 section, respectively. Therefore, these two streams are crucial to the performance of the subsequent sections. L533, L521, and L503 are the key streams connecting the three sections. As shown in Table 12, the calculated composition of L533 generally coincides with the experimental result, but evident discrepancies between the calculated and experimental compositions remain for L521 and L503. The discrepancies are found in the components with lower contents (impurity components), that is, H_2SO_4 in the HI_x phase, and HI and I_2 in the H_2SO_4 phase. The cause of the discrepancy is analyzed as follows.

The accuracy of the measurement decreases with increasing iodine concentration because iodine vapor may escape and some dissolved iodine may also precipitate during the sampling procedure. Considerable errors readily arise when the concentrations of the components with very low contents are measured. In addition, the IS-10 facility might not have reached the steady state at the moment of sampling. In contrast, the simulation converges and achieves steady state. Therefore, discrepancies exist between the calculated and experimental compositions, particularly L521 and L503.

Overall, the calculated H_2 and O_2 flow rates and the set values of the conversion ratios and removal ratios of HI and H_2SO_4 lie exactly within the variation range of the experimental data. Also, the model can accurately predict the compositions of most key streams. The discrepancies are likely caused by the errors in the measurement. Hence, the simulation model for the I-S process is considered reliable.

Parameter sensitivity analysis

In the hydrogen production process, some parameters are very sensitive to input duty; a slight variation of the parameter will result in considerable change in the input duty. The most sensitive parameters to the input duty were sought out by sensitivity analysis, and the optimal values for the parameters to lower the total input duty were determined.

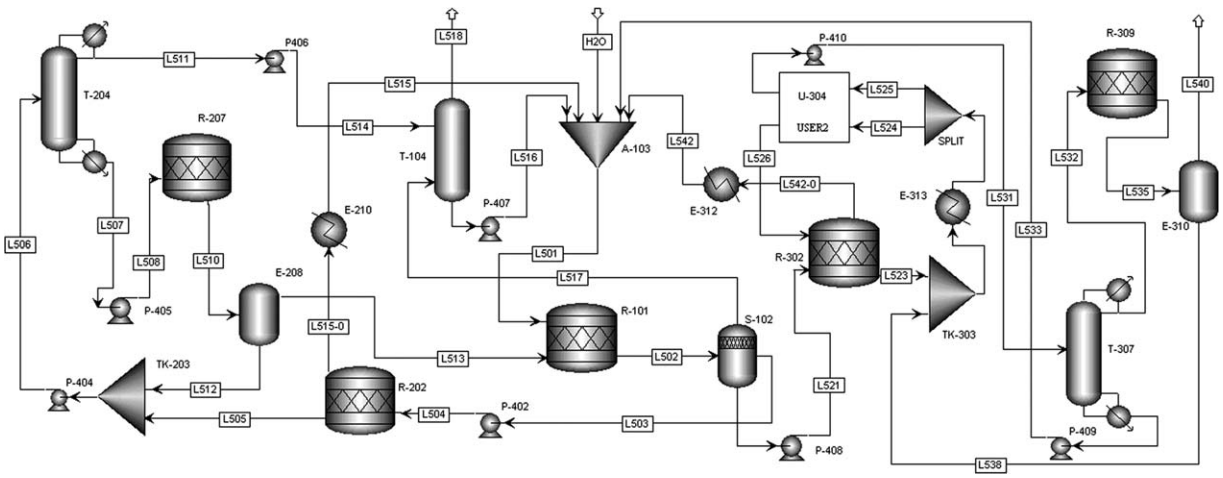

Figure 11. Flow sheet of the I-S process in Aspen plus for simulating the IS-10 facility.

Table 7. Calculated Parameters of the Streams in the Flow Sheet of IS-10

Stream	Location	Temperature (K)	Pressure (MPa)	Flow Rate (mol/h)						
				H_2O	H_2SO_4	H_2	HI	I_2	O_2	SO_2
H_2O	To A-103	293.0	0.1	0.45	0.00	0.00	0.00	0.00	0.00	0.00
L501	From A-103 to R-10	334.7	0.1	16.37	0.00	0.00	1.12	3.68	0.00	0.28
L502	From R-101 to S-102	353.0	0.1	14.97	0.73	0.00	2.58	3.10	0.22	0.00
L503	From S-102 to R-202	353.0	0.1	1.90	0.48	0.00	0.08	0.03	0.00	0.00
L505	From R-202 to TK-203	403.0	0.1	1.60	0.45	0.00	0.00	0.00	0.00	0.00
L506	From TK-203 to T-204	386.5	0.2	2.20	0.57	0.00	0.00	0.00	0.00	0.00
L507	From T-204 to R-207	495.6	0.1	0.20	0.57	0.00	0.00	0.00	0.00	0.00
L510	From R-207 to E-208	1123.0	0.1	0.65	0.13	0.00	0.00	0.00	0.22	0.45
L511	From T-204 to T-104	371.7	0.1	1.99	0.00	0.00	0.00	0.00	0.00	0.00
L512	From E-208 to TK-203	333.0	0.1	0.60	0.13	0.00	0.00	0.00	0.00	0.00
L513	From E-208 to R-101	333.0	0.1	0.05	0.00	0.00	0.00	0.00	0.22	0.44
L515	From R-202 to A-103	306.6	0.1	0.38	0.00	0.00	0.00	0.06	0.00	0.04
L516	From T-104 to A-103	312.1	0.1	2.01	0.00	0.00	0.00	0.00	0.00	0.00
L517	From S-102 to T-104	353.0	0.1	0.03	0.00	0.00	0.00	0.00	0.22	0.00
L518	From T-104	302.9	0.1	0.01	0.00	0.00	0.00	0.00	0.22	0.00
L521	From S-102 to R-302	353.0	0.1	13.04	0.26	0.00	2.52	3.06	0.00	0.00
L523	From R-302 to TK-303	393.0	0.1	43.84	0.01	0.00	6.87	7.01	0.00	0.01
L524	From SPLIT to U-304	338.0	0.1	38.68	0.00	0.00	5.12	3.73	0.00	0.00
L525	From SPLIT to U-304	338.0	0.1	38.68	0.00	0.00	5.12	3.73	0.00	0.00
L526	From U-304 to R-302	373.0	0.1	38.33	0.00	0.00	4.90	3.84	0.00	0.00
L531	From U-304 to T-307	338.0	0.1	39.03	0.00	0.00	5.33	3.62	0.00	0.00
L532	From T-307 to R-309	389.7	0.1	33.53	0.00	0.00	4.26	0.00	0.00	0.00
L533	From T-307 to A-103	404.1	0.1	5.49	0.00	0.00	1.07	3.62	0.00	0.00
L535	From R-309 to E-310	723.0	0.1	33.53	0.00	0.45	3.37	0.45	0.00	0.00
L538	From E-310 to TK-303	313.0	0.1	33.51	0.00	0.00	3.37	0.45	0.00	0.00
L540	From E-310	313.0	0.1	0.02	0.00	0.45	0.00	0.00	0.00	0.00
L542	From R-302 to A-103	290.9	0.1	8.02	0.00	0.00	0.05	0.03	0.00	0.25

Table 8. Flow Rates of the Products

Flow Rate(NL/h)	H_2	O_2
Experimental data	9.89–10.70	4.76–5.30
Calculated value	10.00	5.00

Parameter Analysis of the H_2SO_4 Section. Figure 12 displays the variation trend of the total input duty of the H_2SO_4 section when parameters are altered around their basic values. Total input duty is positively correlated with the ratio of the distillate to the feed rate and reflux ratio but negatively correlated with the conversion ratio of H_2SO_4. The slopes of the curves indicate how strongly the variations of the parameters influence input duty. When the parameters are greater than their basic values, the ratio of distillate rate to feed rate is the most sensitive factor to the duty of the H_2SO_4 section per mol H_2 throughput; whereas, the conversion ratio of H_2SO_4 becomes the most sensitive factor when the parameters decrease to values lower than their basic values. The reflux ratio is always insensitive to the variation of the duty of the H_2SO_4 section compared with the other two factors.

The two sensitive parameters should be paid more attention during the operation. The ratio of distillate rate to feed rate should be maintained less than the basic value, that is, 0.75, because the input duty increases sharply when this ratio exceeds the basic value. On the other hand, a higher H_2SO_4 conversion ratio signifies lower input duty. However, in the actual operation, the highest H_2SO_4 conversion ratio that can be achieved ranges from 0.75 to 0.78; thus, the conversion ratio should be retained not less than the basic value, which is 0.75.

The total input duty per unit of hydrogen rate exhibits different variation trends as the ratio of distillate rate to feed rate changes from less than the basic value to more than the value. This behavior is attributed to the variation in the reboiler duty per unit of H_2SO_4 flow rate in the bottom product of the H_2SO_4 distillation column, which contributes to the total heat duty per unit of hydrogen rate in the H_2SO_4 section. When the ratio of distillate rate to feed rate is less than the basic value, that is, 0.75, the distillate is pure water, and all H_2SO_4 remains in the bottom product. The variation of the distillate rate over feed rate causes a small change in the reboiler duty per unit of H_2SO_4 flow rate in the bottom product. However, H_2SO_4 appears in the distillate when the distillate rate over feed rate is greater than 0.75. Large reboiler duty is required to allow the H_2SO_4 to reach the top of the column. The H_2SO_4 flow rate in the bottom product also decreases. As a result, the reboiler duty per unit of H_2SO_4 flow rate in the bottom product increases sharply as the distillate rate over feed rate increases over the basic value of 0.75, which results in the variation trend shown in Figure 12.

Parameter Analysis of the HI Section. Figure 13 presents the effects of the parameters on the input duty of the HI section. The input duty initially decreases then increases as the HI mole fraction in the distillate increases regardless of

Table 9. Comparison of the Setting Values of Conversion and Removal Ratios with Experimental Values

	HI Conversion Ratio	H_2SO_4 Conversion Ratio	HI Removal Ratio in H_2SO_4 Phase	H_2SO_4 Removal Ratio in HI_x Phase
Setting value	0.21	0.78	0.98	0.97
Experimental value	0.18–0.22	0.78–0.80	0.96–0.98	0.97–0.98

Table 10. Compositions of the Outlet Streams of Key Process units (I)

	EED Cathode Outlet Stream (L531)		Distillate of HI Distillation Column (L532)	
Mole Fraction	Calculated Value	Experimental Value	Calculated Value	Experimental Value
x_{HI}	0.11	0.11	0.11	0.12
x_{I2}	0.08	0.03	0.00	0.00
x_{H2SO4}	0.00	0.00	0.00	0.00
x_{H2O}	0.81	0.86	0.89	0.88

Table 11. Compositions of the Outlet Streams of Key Process Units (II)

Mass Fraction of H_2SO_4	Bottom Product of H_2SO_4 Distillation Column (L507)
Calculated value	0.93
Experimental value	0.92–0.94

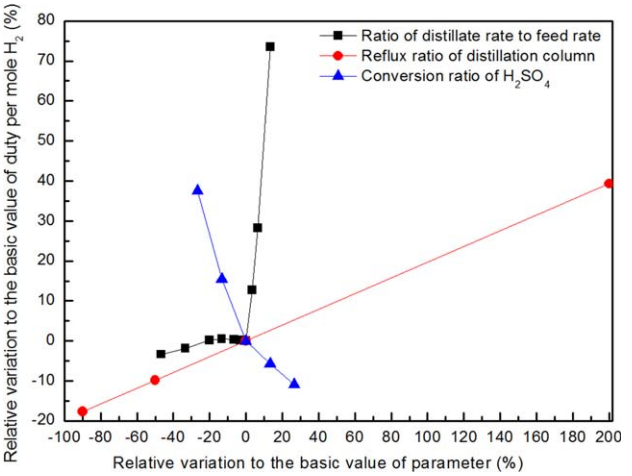

Figure 12. Sensitivity analysis of the parameters in H_2SO_4 section.

[Color figure can be viewed in the online issue, which is available at wileyonlinelibrary.com.]

whether a liquid or vapor phase distillate is adopted. The HI molality in EED cathode outlet stream is the most sensitive factor to input duty among the three parameters. Input duty declines monotonously as HI molality increases within the concentration range of interest.

In the operation of the I-S process, more attention should be paid to the adjustment of HI molality in the EED cathode outlet stream. Although the increase in HI molality can diminish input duty effectively, the increase is not limitless. Yoshida et al.[36] reported that the difference in the HI molality between the catholyte and anolyte of the EED will not exceed 5 mol/kg-H_2O because H_2O permeation through the membrane is faster when a large HI molality difference between the two cell compartments is presented; HI molality cannot exceed the limit because of the dilution caused by the permeated H_2O. Therefore, the optimal value for HI molality is obtained when it increases to allow the molality difference to equal 5 mol/kg-H_2O. The optimal value of HI molality in EED cathode outlet stream is the basic value selected in the present study, that is, 11.05 mol/kg-H_2O.

The variation trend of the input duty with increasing HI mole fraction in liquid (or vapor) distillate is nonmonotonic. The input duty can reach the minimum at a certain value of the HI mole fraction, which is likely the optimal value of the parameter. However, implementability should also be considered in the practical operation. Although input duty reduces to a minimum value when the HI mole fraction in a liquid distillate is 17.4% greater than its basic value, the corresponding bubble point of the distillate is 276 K at 0.1 MPa, which requires a special and expensive coolant for condensation. If the HI mole fraction is adjusted back to its basic value, that is, 0.23, the duty increases by 6.8%; the bubble point increases to around 323 K, and the normal cooling water is deemed adequate. Considering both input duty and implementability, a compromise was established and the basic value was selected as the optimal value. When a vapor distillate is employed, the minimum input duty can be obtained at the basic value of the HI mole fraction, that is, 0.3. Under this condition, the dew point of the distillate is 398 K, and air can be utilized for condensation. Thus, the basic value we selected is optimal. As Hodotsuka et al.'s experimental data[37] and Guo et al.'s calculated results[12] indicate, the relative volatility of HI in the HI_x mixture is quite large when the composition is within the overazeotropic region. Therefore, it is possible and not difficult to obtain a distillate with HI mole fraction equaling 0.23, 0.3, or even higher at the top of the HI distillation column at atmospheric pressure, when the feed is concentrated to over azeotropic.

We discovered that applying a vapor distillate is more energy-efficient than applying a liquid distillate to the HI distillation column because much energy can be saved during vaporization in the HI decomposer. A quarter to a third of energy is saved when a vapor distillate is utilized instead of a liquid one.

However, we did not consider the efficiency of heat transfer in our analysis, nor did we consider the optimization of the heat exchange networks in this work. Assessing heat exchange is also important for improving the efficiency, and the simulation program developed in this study can be readily utilized for this purpose. We will investigate these issues in our subsequent research.

Table 12. Compositions of Key Recycled Streams

	Bottom Product of the HI Distillation Column (L533)		HI_x Phase of Bunsen Products (L521)		H_2SO_4 Phase of Bunsen Products (L503)	
Mole Fraction	Calculated value	Experimental value	Calculated value	Experimental value	Calculated value	Experimental value
x_{HI}	0.11	0.11	0.14	0.10	0.03	0.01
x_{I_2}	0.36	0.32	0.16	0.16	0.01	0.00
$x_{H_2SO_4}$	0.00	0.00	0.01	0.01	0.19	0.15
x_{H_2O}	0.54	0.57	0.69	0.73	0.76	0.84

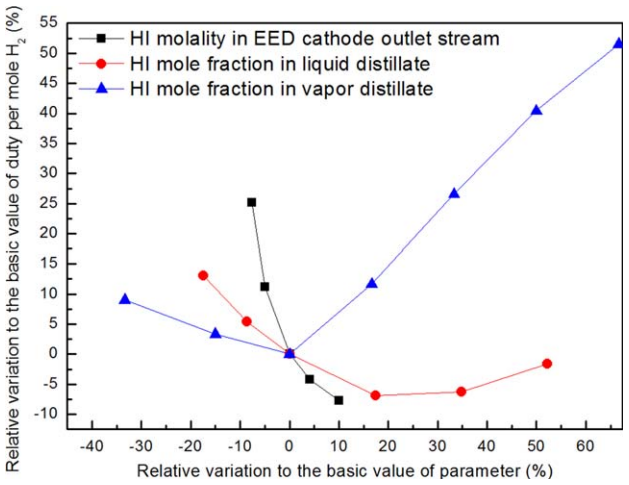

Figure 13. Sensitivity analysis of the parameters in HI section.

[Color figure can be viewed in the online issue, which is available at wileyonlinelibrary.com.]

Conclusions

This article studied the I-S process through commercial software programs Aspen Plus and OLI database, as well as through some self-developed models.

The computer models for the two-phase separator in the Bunsen section and EED were built based on the experimental data. The phase separator model is capable of predicting the compositions and amounts of the two immiscible phases of the Bunsen product mixture when the overall composition of the mixture is provided. The compositions and flow rates of the outlet streams of EED as well as the voltage can be calculated by the EED model when the parameters of the inlet streams and the current density are provided.

The simulation program for the global I-S process was completed based on the two-phase separator and EED models. The reliability of the calculated results was verified by the experimental data from the IS-10 facility.

Sensitivity analyses of some of the important parameters in the H_2SO_4 and HI sections were conducted with the simulation program. Among the evaluated parameters, the ratio of distillate rate to feed rate in the H_2SO_4 distillation column was found to be the most sensitive factor to the input duty of the H_2SO_4 section. The HI molality in the EED cathode outlet stream was found to be the most sensitive factor to the input duty of the HI section. The optimal values of the examined parameters were discussed.

The models and simulation programs developed in this study offer a powerful tool that can analyze the performance and can design the flow sheet of the I-S process. The results of the sensitivity analysis provide guidance in the actual operation of the I-S hydrogen production facility.

Acknowledgment

This work was supported by the National Natural Science Foundation of China (Grant No. 20976092) and the State Key Science and Technology Project (Grant No. zdzx 06901).

Notation

C_i = molarity of component i
E = voltage of EED
M_i = molar mass of component i
R^j = molar ratio of the amount of phase j to that of the mixture
t_+ = transport number of proton (the molar ratio of the proton that permeates through the membrane to the electron that reacts at electrodes)
X_i = overall mole fraction of component i in the mixture of Bunsen products
x_i^j = mole fraction of component i in phase j

Greek letters

β = electroosmosis coefficient (molar ratio of permeated quantities of water and protons)
μ_i = chemical potential of component i
ρ = density

Superscripts

fd = feed
hi = HI_x (polyhydriodic acid) phase
sa = H_2SO_4 phase

Subscripts

mn = the mean value

Literature Cited

1. Russel JL, Jr., McCorkle KH, Norman JH, Porter II JT, Roemer TS, Schuster JR, Sharp RS. Water splitting: a progress report. In: *Proc. 1st World Hydrogen Energy Conf.* Miami Beach, FL, 1976.
2. Norman JH, Besenbruch GE, O'Keefe DR. *Thermochemical Water-Splitting for Hydrogen Production.* Gas Research Institute, Chicago, IL, U.S.A., 1981 GRI-80/0105.
3. Kubo S, Kasahara S, Okuda H, Terada A, Tanaka N, Inaba Y, Ohashi H, Inagaki Y, Onuki K, Hino R. A pilot test plan of the thermochemical water-splitting iodine-sulfur process. *Nucl Eng Des.* 2004;233:355–362.
4. Goldstein S, Borgard JM, Vitart X. Upper bound and best estimate of the efficiency of the iodine sulphur cycle. *Int J Hydrogen Energy.* 2005;30(6):619–626.
5. Bae KK, Park CS, Kim CH, Kang KS, Lee SH, Hwane GJ, Choi HS. Hydrogen production by thermochemical water-splitting IS process. In: WHEC 16. Lyon, France, 2006.
6. Lanchi M, Ceroli A, Liberatore R, Marrelli L, Maschietti M, Spadoni A, Tarquini P. S-I thermochemical cycle: a thermodynamic analysis of the HI-H_2O-I_2 system and design of the HI_x decomposition section. *Int J Hydrogen Energy.* 2009;34(5):2121–2132.
7. Zhang P, Chen S, Wang L, Xu J. Overview of nuclear hydrogen production research through iodine sulfur process at INET. *Int J Hydrogen Energy.* 2010;35(7):2883–2887.
8. O'Keefe D, Allen C, Besenbruch G, Brown L, Norman J, Sharp R. Preliminary results from bench-scale testing of a sulfur-iodine thermochemical water-splitting cycle. *Int J Hydrogen Energy.* 1982;7(5): 381–392.
9. Guo H, Zhang P, Lan S, Chen S, Wang L, Xu J. Study on the phase separation characteristics of HI-I_2-H_2SO_4-H_2O mixture at 20°C. *Fluid Phase Equilib.* 2012;324(25):33–40.
10. Bai Y, Zhang P, Guo H, Chen S, Wang L, Xu J. Purification of sulfuric and hydriodic acids phases in the iodine-sulfur process. *Chin J Chem Eng.* 2009;17(1):160–166.
11. Guo H, Zhang P, Bai Y, Wang L, Chen S, Xu J. Continuous purification of H_2SO_4 and HI phases by packed column in IS process. *Int J Hydrogen Energy.* 2010;35(7):2836–2839.
12. Guo H, Zhang P, Chen S, Wang L, Xu J. Review of thermodynamic properties of the components in HI decomposition section of the iodine-sulfur process. *Int J Hydrogen Energy.* 2011;36(16):9505–9513.
13. Engels H, Knoche KF, Roth M. Direct dissociation of hydrogen iodide: an alternative to the General Atomic proposal. *Int J Hydrogen Energy.* 1987;12(10):675–678.
14. Onuki K, Nakajima H, Shimizu S. Concentration of HIx solution by electrodialysis. *Kagaku Kogaku Ronbun.* 1997;23(2):289–291.
15. Zhang P, Chen S, Wang L, Yao T, Xu J. Study on a lab-scale hydrogen production by closed cycle thermo-chemical iodine-sulfur process. *Int J Hydrogen Energy.* 2010;35(19):10166–10172.

16. Giaconia A, Grena R, Lanchi M, Liberatore R, Tarquini P. Hydrogen/methanol production by sulfur-iodine thermochemical cycle powered by combined solar/fossil energy. *Int J Hydrogen Energy*. 2007;32(4):469–481.
17. Huang CP, T-Raissi A. Analysis of sulfur-iodine thermochemical cycle for solar hydrogen production. Part I: decomposition of sulfuric acid. *Sol Energy*. 2005;78(5):632–646.
18. Belaissaoui B, Thery R, Meyer XM, Meyer M, Gerbaud V, Joulia X. Vapour reactive distillation process for hydrogen production by HI decomposition from HI-I_2-H_2O solutions. *Chem Eng Process*. 2008;47(3):396–407.
19. Elder RH, Priestman GH, Ewan BC, Allen RWK. The separation of HI_x in the sulphur-iodine thermochemical cycle for sustainable hydrogen production. *Process Saf Environ Protect*. 2005;83(B4):343–350.
20. Kane C, Revankar ST. Sulfur-iodine thermochemical cycle: HI decomposition flow sheet analysis. *Int J Hydrogen Energy*. 2008; 33(21):5996–6005.
21. Murphy IV JE, O'Connell JP. Process simulations of HI decomposition via reactive distillation in the sulfur-iodine cycle for hydrogen manufacture. *Int J Hydrogen Energy*. 2012;37(5):4002–4011.
22. Kasahara S, Guo H, Tanaka N, Imai Y, Iwatsuki J, Kubo S, Onuki K. Flowsheet study of HI separation process from HI-H_2O-I_2 solution in the thermochemical hydrogen production iodine-sulfur (IS) process. In: *Proc. 19th International Conference on Nuclear Engineering in Osaka*. Osaka, Japan, 2011.
23. Guo H, Kasahara S, Onuki K, Zhang P, Xu J. Simulation study on the distillation of hyper-pseudo-azeotropic HI-I_2-H_2O mixture. *Ind Eng Chem Res*. 2011;50(20):11644–11656.
24. Guo H, Zhang P, Chen S, Wang L, Xu J. Comparison of various circuit designs in the HI decomposition section of the iodine-sulfur process. *Int J Hydrogen Energy*. 2012;37(17):12097–12104.
25. Brown LC, Besenbruch GE, Lentsch RD, Schultz KR, Funk JF, Pickard PS, Marshall AC, Showalter SK. High Efficiency Generation of Hydrogen Fuels using Nuclear Power Final Technical Report for the Period August 1, 1999 through Sepetember 30, 2002. General Atomics, San Diego, California, U.S.A., 2003. GA-A24285.
26. Mathias PM, Brown LC. Thermodynamics of the sulfur-iodine cycle for thermochemical hydrogen production. In: The 68th Annual Meeting of the Society of Chemical Engineers. Japan, 2003.
27. Kasahara S, Hwang GJ, Nakajima H, Choi HS, Onuki K, Nomura M. Effects of process parameters of the IS process on total thermal efficiency to produce hydrogen from water. *J Chem Eng Jpn*. 2003; 36(7):887–899.
28. Kasahara S, Onuki K, Nomura M, Nakao S. Static analysis of the thermochemical hydrogen production IS process for assessment of the operation parameters and the chemical properties. *J Chem Eng Jpn*. 2006;39(5):559–568.
29. Hadj-Kali MK, Gerbaud V, Lovera P, Baudouin O, Floquet P, Joulia X, Borgard JM, Carles P. Bunsen section thermodynamic model for hydrogen production by the sulfur-iodine cycle. *Int J Hydrogen Energy*. 2009;34(16):6625–6635.
30. Atkins P, De Paula J. *Atkins' Physical Chemistry*, 8th ed. Oxford, UK: Oxford University Press, 2006.
31. Onuki K, Hwang GJ, Arifal, Shimizu S. Electro-electrodialysis of hydriodic acid in the presence of iodine at elevated temperature. *J Memb Sci*. 2001;192(1-2):193–199.
32. Onuki K, Hwang GJ, Shimizu S. Electrodialysis of hydriodic acid in the presence of iodine. *J Membr Sci*. 2000;175(2):171–179.
33. Guo H. *Study on the Process Simulation of Iodine-Sulfur Thermochemical Cycle*. Doctor's Thesis, Institute of Nuclear and New Energy Technology, Tsinghua University, Beijing, P.R. China, 2012.
34. Giaconia A, Caputo G, Ceroli A, Diamanti M, Barbarossa V, Tarquini P, Sau S. Experimental study of two phase separation in the Bunsen section of the sulfur-iodine thermochemical cycle. *Int J Hydrogen Energy*. 2007;32(5):531–536.
35. Lee BJ, No HC, Yoon HJ, Kim SJ, Kim ES. An optimal operating window for the Bunsen process in the I-S thermochemical cycle. *Int J Hydrogen Energy*. 2008;33(9):2200–2210.
36. Yoshida M, Tanaka N, Okuda H, Onuki K. Concentration of HIx solution by electro-electrodialysis using Nafion 117 for thermochemical water-splitting IS process. *Int J Hydrogen Energy*. 2008;33(23): 6913–6920.
37. Hodotsuka M, Yang X, Okuda H, Onuki K. Vapor-liquid equilibria for the HI+H_2O system and the HI+H_2O+I_2 system. *J Chem Eng Data*. 2008;53(8):1683–1687.

Manuscript received Dec. 22, 2012, and revision received Sept. 23, 2013.